Phenomenological model of anomalously high photovoltages generated in obliquely deposited semiconductor films

S. N. Singh[a] and Dinesh Kumar
Division of Electronic Materials, National Physical Laboratory, Dr. K.S. Krishnan Marg, New Delhi-110012, India

(Received 1 July 2007; accepted 30 October 2007; published online 28 January 2008)

Photovoltage in obliquely deposited films of semiconductors is found to be much higher in magnitude than the corresponding band gap of the semiconductor. Also, the magnitude of the photovoltage depends on the angle of deposition, the separation between the electrodes, the wavelength of the incident light, the intensity of the illumination and temperature, but this behavior is not understood well. In this work a phenomenological model of the generation of photovoltage along the horizontal plane of the obliquely deposited films on transparent substrates is presented for the first time. The model is based on the presence of obliquely grown grains separated by parallel grain boundaries and the existence of grain boundary potential barriers across the grain boundaries. In the case of semiconductor films with a high absorption coefficient for short wavelengths in the visible range, there occurs a relatively large photogeneration of carriers on the front side of the grain boundaries rather than on the back side, and this gives rise to a net photocurrent and a photovoltage across each grain boundary. The horizontal components of this photovoltage get added up due to a large number of grain boundaries lying between the electrodes on the front surface and produce a large photovoltage due to the series combination. An expression has been derived based on this model which shows that for low intensities of illumination the horizontal component $\bar{V}_{\mathrm{och}}$ of the photovoltage increases linearly with electrode separation, resistivity of the film, and the incident light intensity. It depends on the angle of deposition and under certain conditions it is expected to be maximum when the angle of deposition is 45°. The analysis can be applied to study the effect of increase in intensity or decrease in temperature on $\bar{V}_{\mathrm{och}}$. It also shows that the photovoltage across the thickness of the obliquely deposited film $\bar{V}_{\mathrm{ocv}}$ is minimum for normal deposition and increases with the increase in the angle of oblique deposition. © *2008 American Institute of Physics*.
[DOI: 10.1063/1.2828009]

I. INTRODUCTION

Photovoltages, much larger than the band-gap energy (E_g) of the semiconductor, have been observed in obliquely deposited thin films of a large number of semiconductors[1–14] on transparent substrates under normal illumination. This effect is commonly known as the anomalous photovoltaic effect (APV). The first observation of the APV effect was made by Starkienicz, Sosnowski, and Simpson in 1946 in PbS films[1] and was confirmed later by Berlaga and co-workers,[2,3] Schwabe[4] and Piwkowski.[5] Goldstein and Pensak[6–9] discovered unusually high photovoltages in some CdTe films made by vacuum deposition. The magnitude of photovoltage was related with the direction of evaporation and a value as high as 100 V cm^{-1} was obtained in sunlight. Extensive studies[1–24] of a range of materials have established beyond a doubt that a necessary condition for the appearance of the anomalous photovoltage (APV) is that the semiconductor material should be evaporated onto a substrate at an angle to the normal leading to skewed columnar growth.[8] However, the precise conditions under which successful APV structures may be obtained are far from clear and it has been difficult to obtain reproducible results.[8] Kallmann *et al.*,[12] during their studies on Ge and Si films of ~1 μm thickness formed by vacuum evaporation, observed that generally the absolute value of the photovoltage measured between two metal contacts separated by 1 cm was larger at lower temperature. They found 1250 V at liquid nitrogen temperature. However, the short-circuit currents were low: $\sim 5.5\times 10^{-9}$ A at room temperature, and decreased further to 3×10^{-9} A at low temperatures. The photovoltages were proportional to the light intensity and only in the case of very large photovoltages was the increase with intensity less than linear. They tried to explain the results qualitatively in terms of the Dember effect.

A systematic study of the dependence of APV on the wavelength and intensity of incident light and the temperature was made by Brandhorst *et al.*[10,13] in thin films of CdS, Si, and SiC. The CdS films were deposited on a quartz substrate at an angle of 45° from the normal. The substrate temperature was 280–370 °C and the average thickness of the films was between 10 and 200 nm. The photovoltages were measured under a tungsten filament light of 150 $\mathrm{mW/cm}^2$ intensity. They found reproducible fabrication of high photovoltage films difficult. Only two films displayed high photovoltages, 17 and 12 V, at room temperature. However, at the sufficiently low temperature most of the films exhibited pho-

[a]Author to whom correspondence should be addressed. Tel: +91-11-25734283. FAX: +91-11-25726938. Electronic mail: snsingh@mail.nplindia.ernet.in.

tovoltages larger than the corresponding band gaps. The spectral response of photovoltage was of an inverted-V shape with a peak at ~500 nm wavelength.[10] Photovoltage varied linearly with intensity up to 50 mW/cm^2 but increased at a smaller rate between 50 and 150 mW/cm^2 intensity.[10] In CdS films[10] and also in a Si film,[13] the photovoltage increased with the decrease in temperature from 330 to ~230 K and then decreased with further lowering of the temperature.[13] They tried to attribute the occurrence of large photovoltages to the existence of multiple trapping levels. Degradation of the photovoltage due to exposure in air was observed and was attributed to the surface absorption of oxygen, which produces surface states.

Patel and Patel[23] deposited $AgInTe_2$ films at different inclinations from the normal and found that the photovoltage depended on the deposition angle and was maximum for the films deposited at 45°. The magnitude of the peak photovoltage varied with the substrate temperature. They observed that the angle of deposition introduced an asymmetric growth of crystallites, and the asymmetry was maximum for 45°.[23] The occurrence of APV was explained by assuming the presence of a p-p^+ junction at each crystallite that generated a small photovoltage, and the number of aligned p-p^+ junctions being connected in series gave a large photovoltage. Similarly, the occurrence of a high photovoltage in the other obliquely deposited semiconductor films has been explained qualitatively assuming a series of micro p-n junctions or p-p^+ or n-n^+ junctions, each capable of generating a small photovoltage.[22]

Despite a large amount of experimental data and many attempts to explain them, a picture of APV is not yet clear. A comprehensive model that may provide an explanation of the observed high photovoltages and their dependence on intensity of light, wavelength of light, temperature, the angle of deposition, etc., is very much desired. In this paper we present a phenomenological model of the generation of high photovoltages in obliquely deposited semiconductor films and apply it to explain all observations of earlier researchers for silicon films.

II. THEORETICAL MODEL

Guided by the various observations of researchers discussed above, we develop in the following a phenomenological model based on the following basic assumptions. We assume that the oblique angle deposition of semiconductor films on heated transparent substrates in vacuum gives rise to columnar polycrystalline grains which grow in the direction of the deposition, i.e., the semiconductor films contain obliquely grown columnar grains of equal thickness separated by grain boundaries (GB) between them, and all grain boundaries are parallel to each other and are inclined with respect to the horizontal. Under thermal equilibrium there exists a double potential barrier at each grain boundary due to the trapping of majority carriers at GB. This leads to a depletion layer of appreciable thickness "w" on each side of the grain boundary. There exists a built-in-electric field in the depletion region that tries to pull the photogenerated minority carriers toward the grain boundary from each of the two

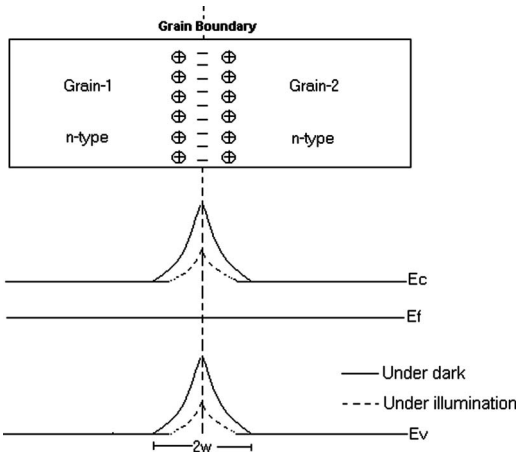

FIG. 1. Grain boundary potential double barriers in an n-type semiconductor film under dark and uniform illumination.

grains. In the present analysis we assume that the film is n-type, although the analysis should be applicable equally to p-type films also. Thus, the photogenerated holes of each grain recombine with the trapped charges at GB and reduce the potential barrier as shown in Fig. 1 and consequently generate a photovoltage between the GB and the grain. The net photovoltage between the two adjacent grains, if any, can be due to the differences in the photovoltages developed across the two sides of the GB. Henceforth we shall refer to photovoltage as the voltage at the open-circuit condition unless mentioned otherwise.

Let us consider that a semiconductor film is deposited obliquely on a substrate B_1B_2 from a source S, where SM represents the direction of normal deposition as shown in Fig. 2. SB_1 and SB_2 subtend angles β_1 and β_2, respectively, with normal SM. We further assume that B_1B_2 is small in comparison with MB_2, and the difference in β_1 and β_2 is negligibly small such that $\beta_1 \approx \beta_2 = \beta$; consequently, the grown films have columnar grains of equal thickness and grain boundaries are inclined at an angle $\theta = 90° - \beta$ with the horizontal.

Figure 3 shows an obliquely deposited semiconductor film on substrate B_1B_2 with the deposited film on top. Here, G_0, G_1 , and G_2 mark grain boundaries, which make the

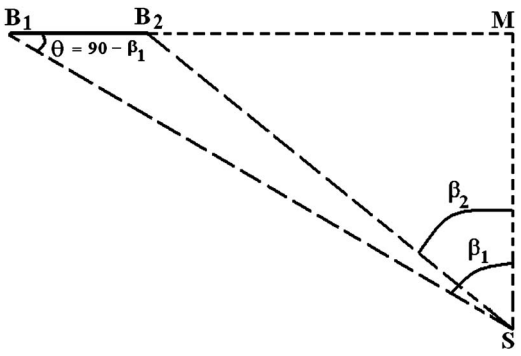

FIG. 2. Schematic diagram of oblique angle deposition of film on substrate B_1B_2. S is the source and β_1 and β_2 are the angles the lines SB_1 and SB_2 make with the normal SM. Angle $SB_1M = \theta = 90 - \beta_1$. When $B_1B_2 \ll MB_2$, then $\beta_1 \approx \beta_2 = \beta$ and $\theta = 90 - \beta$.

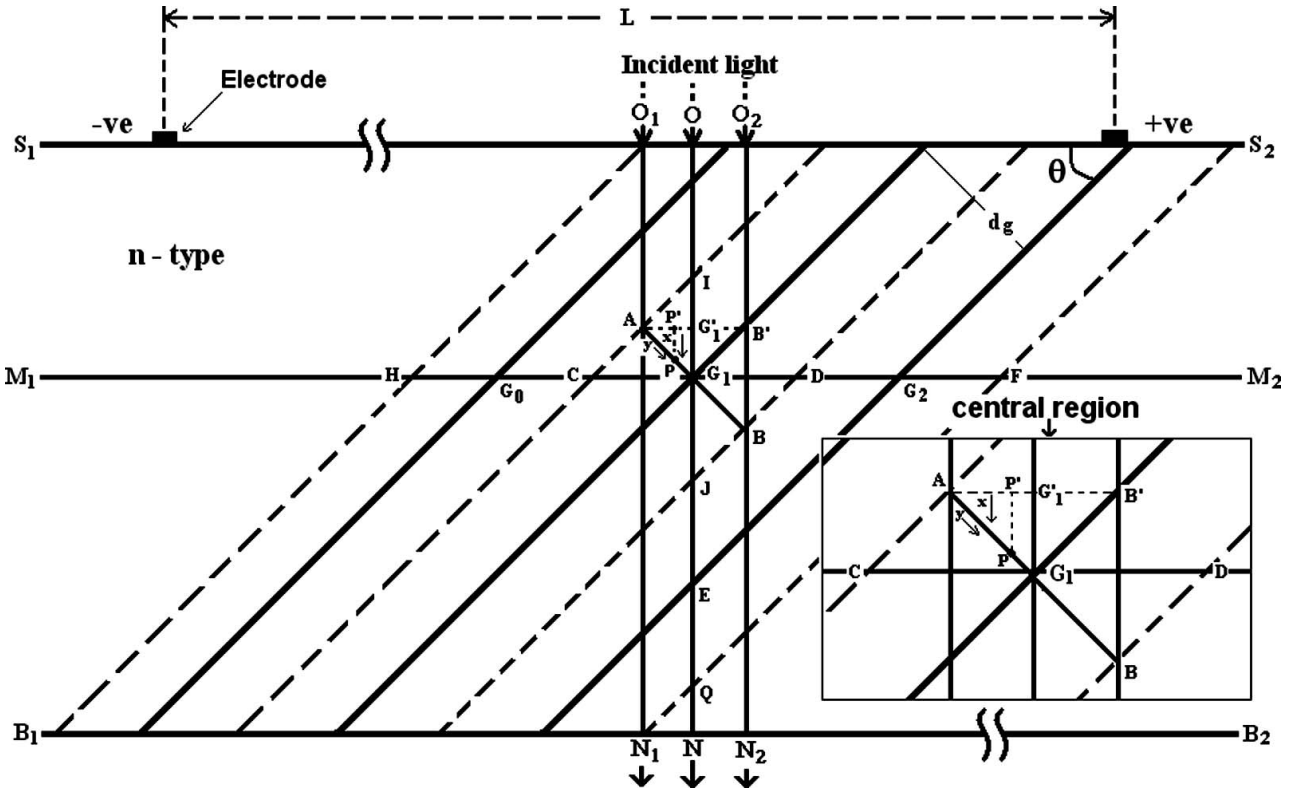

FIG. 3. Schematic diagram of *n*-type grains, grain boundaries, and depletion layers formed in the obliquely deposited semiconductor films on a transparent substrate B_1B_2. G_0, G_1, G_2 are parallel grain boundaries. S_1S_2 is the front surface of the film. ON is normal to S_1S_2 and is the direction of the light travel in the film. In the case of partially depleted grains, AG_1, G_1B are larger than the width of the depletion layer "w" on each side of the grain boundary. AP', AG'_1, and AB' are the horizontal projections of AP, AG_1, and AB, respectively. $O_1A=OG'_1=O_2B'=r$. Inset shows the enlarged central region.

angle θ with the front horizontal surface S_1S_2. Now, we make the following specific assumptions:

(1) All grain boundaries of Fig. 3 are parallel to each other and spread from the front surface to the bottom end of the films touching the substrate. This means all grains are single crystalline and are of equal thickness (d_g) when measured in the direction perpendicular to the grain boundaries.
(2) Majority carriers of the grains are trapped at the grain boundaries due to the existence of a large interface state density of traps at the GBs. This results in full or partial depletion of grains and creation of grain boundary potential barriers at GBs as shown in Fig. 1.
(3) The film is illuminated normally from the front side and the light beams travel in film in the direction ON or parallel to ON (i.e., along O_1N_1, O_2N_2, etc.). We also assume the optical properties such that the refractive index and absorption coefficient α_λ of light for any given wavelength λ is not affected by the presence of dopant impurities or grain boundaries. The substrate is transparent to light and the unabsorbed light is not reflected back into the film.
(4) The photogeneration of carriers takes place along the direction (ON) of travel of the light rays in the film. However, the collection of photogenerated carriers takes place in the direction of the normal (AB) to the grain boundaries due to the built-in electric field in the depletion layer of the grain. In Fig. 3 we consider the collection of the photogenerated minority carriers from the two sides of the grain boundary G_1. The collection of photogenerated holes along AG_1 in the grain on the front side will give a short-circuit current density J_{scf1}. Similarly, the photogenerated holes along G_1B in the grain on the bottom side of G_1 will give a short-circuit current density J_{scb1}. The difference of j_{scf1} and J_{scb1} will be the resultant short-circuit current density responsible for generation of photovoltage across G_1.

We define the following parameters to derive a relation for a photovoltage across the two electrodes on the horizontal plane along S_1S_2:

L is distance between the electrodes on the front surface.
t is thickness of the deposited film
d_g is the grain size (i.e., the perpendicular distance between the two grain boundaries).
N_d is the dopant density in the grain.
N_{is} is the density of interface states at the grain boundary.
V_B is the height of potential barrier at grain boundary:
$V_B=qd_g^2N_D/(8\varepsilon\varepsilon_o)$ for fully depleted grains,[25] or
$V_B=qN_{\text{is}}^2/(8\varepsilon\varepsilon_oN_d)$ for partially depleted grains.[25]
w_1, w_2 is the width of the grain boundary space-charge layer on the front, back side layer, $w_1 \sim w_2 \sim \varepsilon\varepsilon_oE_b/(qN_D)$, where E_b is the maximum field at GB potential maximum.
P_{in} is the intensity of illumination.
α_λ is the absorption coefficient of light of wavelength λ in the semiconductor.

k is the Boltzmann constant.
q is the electron charge.
c is the velocity of light in vacuum.
n_i is the density of intrinsic carriers.
R_λ is the reflectivity of the front surface S_1S_2 receiving the light of wavelength λ.
n_L is the number of grain boundaries between the two contacts on the horizontal surface.
n_t is the number of grain boundaries between the top and back surface of the film of thickness t.
n_{pho} is the incident photon flux of wavelength λ at the front surface at $r=0$.
λ_g is the cutoff wavelength of the light for absorption in the semiconductor.
n_o is the equilibrium density of majority carriers in the grains.
ρ_g is the resistivity of the semiconductor film.
V_{oc1} is the open-circuit voltage across a grain boundary.
J_{sc1} is the short-circuit current density across a grain boundary.
J_{d1} is the dark current density of a grain boundary potential barrier.
$\bar{V}_{\text{och}}$ is the average V_{oc} developed between the two electrodes on the horizontal plane of the substrate separated by a distance L.
$\bar{V}_{\text{ocv}}$ is the average V_{oc} across the film thickness.

A. Expression for J_{sc1}

We consider the case of photogeneration for grain boundary G_1 at a vertical distance r from the front surface S_1S_2 (at $r=0$). We assume that the grain size d_g is small such that all holes generated over the thickness AG_1 and G_1B contribute to J_{scf1} and J_{scb2}, respectively. This condition can easily be satisfied in practice if the grains are fully depleted and thus have a built-in field all along the thickness AG_1 (or G_1B) of the grain. The condition can be satisfied in the case of a partially depleted grain also if AG_1 (or G_1B) is smaller than the diffusion length of the minority carriers in the grain. The photon flux at point A, at a normal distance r (i.e., O_1A) from the front surface of the film, is given by

$$n_{phr} = n_{pho}(1 - R_\lambda)\exp(-\alpha_\lambda r). \tag{1}$$

As the incident light intensity is the same at all points on S_1S_2 and the light travels normally in the film, the photon flux at a point P on the line AG_1 lying at a vertical distance $(r+x)$ from the surface SS_1 can be obtained as

$$n_{phy} = n_{phr}\exp(-\alpha_\lambda x), \tag{2}$$

where x is the distance of P from point A in the direction parallel to ON and y is the distance of P from A in the AG_1 direction. Therefore, $x=y\cos\theta$. It may be pointed out that x and y are not the usual orthogonal axes. They simply represent distances from point A along the ON and AG_1 directions, respectively.

At point G_1 we have $x=(d_g/2)\cos\theta$ and $y=d_g/2$. Therefore, along the AG_1, the photon flux at P will be given by

$$n_{phy} = n_{phr}\exp(-\alpha_\lambda y\cos\theta). \tag{3}$$

Defining $\alpha_\lambda\cos\theta=\alpha_y$, the photon flux at any point P along the direction y can be written as

$$n_{phy} = n_{phr}\exp(-\alpha_y y). \tag{4}$$

If J_{scf1} is the short-circuit current density due to a collection of holes along the direction AG_1, then, ignoring the recombination term, we can write

$$\frac{1}{q}\frac{dJ_{\text{scf1}}}{dy} = \alpha_y n_{phr}\exp(-\alpha_y y). \tag{5}$$

Therefore, the short-circuit current density J_{scf1} along AG_1 is given by

$$J_{\text{scf1}} = \int_{y=0}^{y=d_g/2} q\alpha_y n_{phr}\exp(-\alpha_y y)dy. \tag{6}$$

Solving the integral, we obtain

$$J_{\text{scf1}} = qn_{phr}\left\{1 - \exp\left(-\alpha_\lambda\cos\theta\times\frac{d_g}{2}\right)\right\}. \tag{7}$$

Similarly, the short-circuit current density along BG_1 can be written as

$$J_{\text{scb1}} = qn_{phr}\exp\left(-\alpha_\lambda\cos\theta\times\frac{d_g}{2}\right)\times\left\{1 - \exp\left(-\alpha_\lambda\cos\theta\times\frac{d_g}{2}\right)\right\}. \tag{8}$$

The net short-circuit current density J_{sc1}, across the grain boundary G_1, along AB is the difference of Eqs. (7) and (8). Thus, subtracting Eq. (8) from Eq. (7) and substituting Eq. (1) in the resultant equation, we obtain

$$J_{\text{sc1}} = qn_{\text{pho}}(1 - R_\lambda)\exp(-r\alpha_\lambda)\times\left\{1 - \exp\left(-\alpha_\lambda\cos\theta\times\frac{d_g}{2}\right)\right\}^2. \tag{9}$$

For multiwavelength incident light, Eq. (9) can be written as

$$J_{\text{sc1}} = \sum_{\lambda=0}^{\lambda=\lambda_g} qn_{\text{pho}}(1 - R_\lambda)\exp(-r\alpha_\lambda)\times\left\{1 - \exp\left(-\alpha_\lambda\cos\theta\times\frac{d_g}{2}\right)\right\}^2. \tag{10}$$

B. Expression for J_{d1}

For the dark current density J_{d1} across the grain boundary G_1, one can write

$$J_{d1} = J_{o1}\left(\exp\frac{qV_1}{kT} - 1\right) + J_{o2}\left(\exp\frac{qV_1}{2kT} - 1\right). \tag{11}$$

The first term on the right-hand side represents majority carrier current density due to thermionic emission and diffusion of majority carriers across the double barrier at the GB under a forward bias of voltage V_1. The second term on the right-hand side of Eq. (11) is due to the recombination of photo-

generated minority carriers in the space-charge region of the double barrier. The two pre-exponential constants J_{o1} and J_{o2} can be expressed as[26]

$$J_{o1} = \frac{qn_o v_r}{1 + \frac{v_r}{v_d}} \exp\left(\frac{-qV_B}{kT}\right). \tag{12}$$

Here, v_r and v_d are, respectively, the recombination velocity and diffusion velocity of the carriers at the grain boundary potential maxima, and V_B is the grain boundary barrier height. The expression for v_r depends on temperature and effective mass m of majority carriers according to the relation[26]

$$v_r = \sqrt{\frac{kT}{2\pi m}}, \tag{13}$$

and $v_d = \mu_n E_b$ near the grain boundary potential maxima. Here, μ_n is the mobility of the majority carrier electrons and E_b is the maximum field at the GB potential maxima and is given by[26]

$$E_b = \left[\frac{2N_d kT}{\varepsilon\varepsilon_o}\left\{\frac{qV_B}{kT} - 1 + \exp\left(\frac{-qV_B}{kT}\right)\right\}\right]^{1/2}. \tag{14}$$

The pre-exponential constant in the second term on the right-hand side of Eq. (11) is given by

$$J_{o2} = \frac{qn_i}{\tau} w, \tag{15}$$

where τ is the lifetime of the minority carriers in the depletion region of the GB.

For most of the films it can be assumed that $J_{01} \gg J_{02}$, so we have

$$J_{d1} \approx J_{o1} \exp\left(\frac{qV_1}{kT} - 1\right). \tag{16}$$

Now, the net current density J_1 at G_1 across the grain boundary G_1 can be written as

$$J_1 = J_{sc1} - J_{d1}. \tag{17}$$

C. Photovoltage along the horizontal plane

Under the open-circuit condition ($J_1 = 0$) the substitution of expressions for J_{sc1} and J_{d1} from Eqs. (10) and (16), respectively, in Eq. (17) gives the open-circuit voltage V_{oc1} across the grain boundary G_1 in the direction AB (perpendicular to the grain boundary).

Therefore, we have

$$V_{oc1} = \frac{kT}{q} \ln\left(\frac{J_{sc1}}{J_{o1}} + 1\right). \tag{18}$$

For a low level of intensity of illumination, such that $J_{sc1} \ll J_{o1}$, the open-circuit voltage V_{oc1} across the grain boundary G_1 would be given by

$$V_{oc1} = \frac{kT}{q} \times \frac{J_{sc1}}{J_{o1}}. \tag{19}$$

Substituting the values of J_{sc1} and J_{o1} from Eqs. (10) and (12), respectively, in Eq. (19), we will get the open-circuit voltage across a grain boundary given by

$$V_{oc1} = \frac{kT}{qn_o v_r}\left(1 + \frac{v_r}{v_d}\right)\sum_{\lambda=0}^{\lambda_g} n_{pho}(1 - R_\lambda) \times \exp(-r\alpha_\lambda)\left\{1 - \exp\left(-\frac{\alpha_\lambda d_g \cos\theta}{2}\right)\right\}^2 \exp\left(\frac{qV_B}{kT}\right). \tag{20}$$

We have that $\rho_g = 1/qn_o\mu_n$ is the grain resistivity and $P_{in} = n_{pho}hc/\lambda$. Generally $v_r \gg v_d$; then, the open-circuit voltage V_{oc1} across the grain boundary G_1 can be expressed in terms of grain resistivity ρ_g and the light intensity P_{in} as

$$V_{oc1} = \frac{kT\rho_g}{hcE_b}\exp\left(\frac{qV_B}{kT}\right)\sum_{\lambda=0}^{\lambda g} \lambda P_{in}(1 - R_\lambda) \times \exp(-r\alpha_\lambda)\left\{1 - \exp\left(-\frac{\alpha_\lambda d_g \cos\theta}{2}\right)\right\}^2. \tag{21}$$

The horizontal component V_{och1} of V_{oc1} along CD is given as $V_{och1} = V_{oc1} \sin\theta$. At the same distance r from the front surface S_1S_2, identical photovoltage will be developed across other grain boundaries G_0, G_2, etc. So, if there are n_L grain boundaries between the two horizontal electrodes separated by a distance L, the total resultant open-circuit voltage will be given by

$$V_{och} = n_L V_{oc1} \sin\theta. \tag{22}$$

From Fig. 3, we know that n_L and n_t are given by

$$n_L = \frac{L}{d_g}\sin\theta, \tag{23}$$

$$n_t = \frac{t}{d_g}\cos\theta. \tag{24}$$

Therefore, the photovoltage developed between the horizontal electrodes is given by

$$V_{och} = \frac{kT\rho_g L}{hcE_b d_g}\exp\left(\frac{qV_B}{kT}\right)\sum_{\lambda=0}^{\lambda g} \lambda P_{in}(1 - R_\lambda) \times \exp(-r\alpha_\lambda)\left\{1 - \exp\left(-\frac{\alpha_\lambda d_g \cos\theta}{2}\right)\right\}^2 \sin^2\theta. \tag{25}$$

On averaging the value of V_{och} across the entire thickness or the length of the grain boundary, the photovoltage across the horizontal electrodes would be given by

$$\bar{V}_{och} = \frac{\int_0^t V_{och} dr}{\int_0^t dr}. \tag{26}$$

Using Eq. (25) in Eq. (26), we can obtain $\bar{V}_{och}$ for the condition $J_{sc1}/J_{o1} \ll 1$ as

$$\bar{V}_{\mathrm{och}} = \frac{kTL\rho_g}{\alpha_\lambda hcE_b t d_g} \exp\left(\frac{qV_B}{kT}\right) \sum_{\lambda=0}^{\lambda g} \lambda P_{\mathrm{in}}(1-R_\lambda) \times \{1-\exp(-\alpha_\lambda t)\} \left\{1-\exp\left(-\frac{\alpha_\lambda d_g \cos\theta}{2}\right)\right\}^2 \sin^2\theta. \tag{27}$$

D. Dependence of $\bar{V}_{\mathrm{och}}$ on θ

Equation (27) shows that $\bar{V}_{\mathrm{och}}$ depends on the angle θ of grain boundaries from the horizontal surface S_1S_2 and thus on the angle of deposition $\beta=90-\theta$. If the product of the grain size and the absorption coefficient of the film is small such that $\frac{1}{2}d_g\alpha_\lambda \cos\theta \ll 1$, then the photovoltage developed between the horizontal electrodes can be written as

$$\bar{V}_{\mathrm{och}} = \frac{kTL\rho_g}{16hctE_b} \exp\left(\frac{qV_B}{kT}\right) \sum_{\lambda=0}^{\lambda g} \lambda P_{\mathrm{in}}(1-R_\lambda) \times \{1-\exp(-\alpha_\lambda t)\}\alpha_\lambda d_g \sin^2 2\theta. \tag{28}$$

In terms of angle of deposition β, Eq. (28) can be expressed as

$$\bar{V}_{\mathrm{och}} = \frac{kTL\rho_g}{16hctE_b} \exp\left(\frac{qV_B}{kT}\right) \sum_{\lambda=0}^{\lambda g} \lambda P_{\mathrm{in}}(1-R_\lambda) \times \{1-\exp(-\alpha_\lambda t)\}\alpha_\lambda d_g \sin^2 2\beta. \tag{29}$$

Equation (29) shows that $\bar{V}_{och}$ will increase for $0° < \beta < 45°$, attain a maximum value for $\beta=45°$, and will then decrease for $45° < \beta < 90°$.

E. Dependence of $\bar{V}_{\mathrm{och}}$ on apparent resistivity of film

In Eqs. (27)–(29) ρ_g represents the resistivity of the quasineutral grain. The apparent resistivity ρ_a of the film includes the resistivity of the depletion region as well. For a small-grain semiconductor film, the apparent resistivity is given by[25]

$$\rho_a = \rho_g \exp\left(\frac{qV_B}{kT}\right), \tag{30}$$

and the sheet resistance R_{sheet} can be determined as $R_{\mathrm{sheet}} = \rho_a/t$. If the length and the width of the film are equal, then, the R_{sheet} represents the apparent resistance R_a of the film.

In terms of R_{sheet}, Eq. (29) can be written as

$$\bar{V}_{\mathrm{och}} = \frac{kTLR_{\mathrm{sheet}}}{16hcE_b} \sum_{\lambda=0}^{\lambda g} \lambda P_{in}(1-R_\lambda) \times \{1-\exp(-\alpha_\lambda t)\}\alpha_\lambda d_g \sin^2 2\beta. \tag{31}$$

Equation (31) shows that $\bar{V}_{\mathrm{och}}$ will increase with R_{sheet} and hence with R_a linearly.

F. Photovoltage across the thickness of the film

The photovoltage developed at a point G_1, on a grain boundary, at a distance r from the front surface given by Eq. (21) can be rewritten as

$$V_{\mathrm{oc1}} = \sum_{\lambda=0}^{\lambda g} u \exp(-r\alpha_\lambda), \tag{32}$$

where u is given by

$$u = \frac{kT\rho_g\lambda}{hcE_b} \exp\left(\frac{qV_B}{kT}\right) P_{\mathrm{in}}(1-R_\lambda) \times \left\{1-\exp\left(-\frac{\alpha_\lambda d_g \cos\theta}{2}\right)\right\}^2. \tag{33}$$

Now, the vertical component of V_{oc1} along ON, which may be referred to as V_{ocv1}, can be obtained as

$$V_{\mathrm{ocv1}} = V_{\mathrm{oc1}} \cos\theta. \tag{34}$$

Substituting Eq. (32) into Eq. (34), we can write

$$V_{\mathrm{ocv1}} = \sum_{\lambda=0}^{\lambda g} u \cos\theta \exp(-r\alpha_\lambda). \tag{35}$$

Again along the direction ON there is a point E on another grain boundary G_2, which lies at a distance of $d=d_g \sec\theta$ further below G_1. Therefore, the vertical component of the photovoltage generated along ON at the point E can be written as

$$V_{\mathrm{ocv2}} = \sum_{\lambda=0}^{\lambda g} u \cos\theta \exp\{-(r+d)\alpha_\lambda\}. \tag{36}$$

Similarly for the point which may lie just below point E along ON on the next grain boundary, we can write

$$V_{\mathrm{ocv3}} = \sum_{\lambda=0}^{\lambda g} u \cos\theta \exp\{-(r+2d)\alpha_\lambda\}. \tag{37}$$

If there were n_t grain boundaries along the thickness of the film, then total photovoltage generated along the film thickness could be calculated by adding up all the vertical components of the photovoltage generated across individual GBs along the direction ON. Therefore, photovoltage across the thickness of the film is given by

$$V_{\mathrm{ocv}} = V_{\mathrm{ocv1}} + V_{\mathrm{ocv2}} + V_{\mathrm{ocv3}} + \cdots + V_{\mathrm{ocv}n_t}. \tag{38}$$

Substituting the values of V_{ocv1}, V_{ocv2}, etc. in Eq. (38), we have

$$V_{\mathrm{ocv}} = \sum_{\lambda=0}^{\lambda g} u \cos\theta \exp\{-\alpha_\lambda r\}[1+\exp\{-\alpha_\lambda d)\} + \exp\{-\alpha_\lambda 2d)\} + \cdots + \exp\{-\alpha_\lambda (n_t-1)d)\}]. \tag{39}$$

After further solving, Eq. (39) reduces to

$$V_{\mathrm{ocv}} = \sum_{\lambda=0}^{\lambda g} u \cos\theta \exp(-\alpha_\lambda r) \frac{[1-\{\exp(-\alpha_\lambda d)\}^{n_t}]}{1-\exp(-\alpha_\lambda d)}. \quad (40)$$

For $\exp(-\alpha_\lambda d) < 1$ Eq. (40) can be simplified to the first approximation as

$$V_{\mathrm{ocv}} = \sum_{\lambda=0}^{\lambda g} u \cos\theta \exp(-\alpha_\lambda r) \frac{\{1-\exp(-n_t\alpha_\lambda d)\}}{1-\exp(-\alpha_\lambda d)}. \quad (41)$$

Now the average value of V_{ocv}, when r varies from $r=0$ to $r=t$, can be obtained as

$$\bar{V}_{\mathrm{ocv}} = \sum_{\lambda=0}^{\lambda g} u \cos\theta \frac{\{1-\exp(-n_t\alpha_\lambda d)\}\{1-\exp(-\alpha_\lambda t)\}}{\alpha_\lambda t\{1-\exp(-\alpha_\lambda d)\}}. \quad (42)$$

Substituting the value of u from Eq. (33) and $d=d_g \sec\theta$ in Eq. (42), we have

$$\bar{V}_{\mathrm{ocv}} = \frac{kT\rho_g}{hcE_b}\exp\left(\frac{qV_B}{kT}\right)\sum_{\lambda=0}^{\lambda g}\lambda P_{\mathrm{in}}(1-R_\lambda) \times\left\{1-\exp\left(-\frac{\alpha_\lambda d_g\cos\theta}{2}\right)\right\}^2 \times\frac{\{1-\exp(-n_t\alpha_\lambda d_g\sec\theta)\}\{1-\exp(-\alpha_\lambda t)\}}{\alpha_\lambda t\{1-\exp(-\alpha_\lambda d_g\sec\theta)\}}\cos\theta. \quad (43)$$

Again, if $\frac{1}{2}d_g\alpha_\lambda\cos\theta \ll 1$, then Eq. (43) is modified to give

$$\bar{V}_{\mathrm{ocv}} = \frac{kT\rho_g d_g^2}{4hctE_b}\exp\left(\frac{qV_B}{kT}\right)\sum_{\lambda=0}^{\lambda g}\lambda\alpha_\lambda P_{\mathrm{in}}(1-R_\lambda) \times\frac{\{1-\exp(-n_t\alpha_\lambda d_g\sec\theta)\}\{1-\exp(-\alpha_\lambda t)\}}{\{1-\exp(-\alpha_\lambda d_g\sec\theta)\}}\cos^3\theta. \quad (44)$$

In terms of the angle of deposition β, Eq. (44) can be expressed as

$$\bar{V}_{\mathrm{ocv}} = \frac{kT\rho_g d_g^2}{4hctE_b}\exp\left(\frac{qV_B}{kT}\right)\sum_{\lambda=0}^{\lambda g}\lambda\alpha_\lambda P_{\mathrm{in}}(1-R_\lambda) \times\frac{\{1-\exp(-n_t\alpha_\lambda d_g\,\mathrm{cosec}\,\beta)\}\{1-\exp(-\alpha_\lambda t)\}}{\{1-\exp(-\alpha_\lambda d_g\,\mathrm{cosec}\,\beta)\}}\sin^3\beta. \quad (45)$$

Equation (45) shows that along the film thickness $\bar{V}_{\mathrm{ocv}}$ will be minimum for $\beta=0$, i.e., for normal deposition, and will increase for oblique deposition, i.e., $0° < \beta < 90°$.

III. RESULTS AND DISCUSSION

A. Special case when $J_{sc1} \ll J_{o1}$

Equation (28) holds well for $J_{\mathrm{sc1}} \ll J_{o1}$ and shows that for a low level of intensity of illumination the photovoltage $\bar{V}_{\mathrm{och}}$ between the two electrodes placed on the horizontal surface of the obliquely deposited semiconductor film will show the following characteristics:

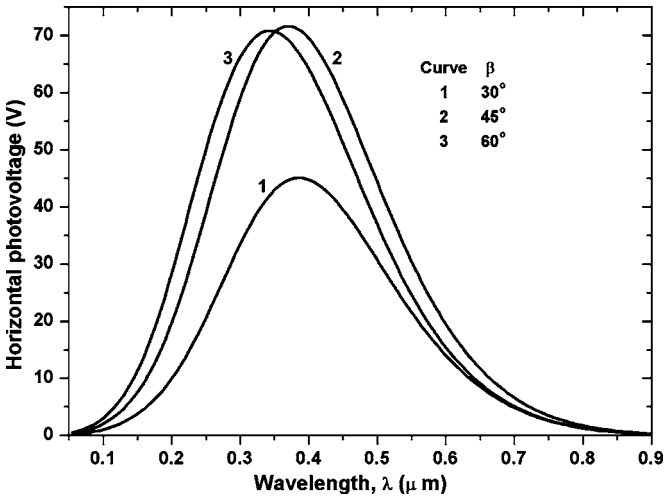

FIG. 4. Variation in photovoltage $\bar{V}_{\mathrm{och}}$ along the horizontal plane S_1S_2 with wavelength λ of incident light of silicon films for three different angles of depositions. The intensity for radiations of different wavelengths is assumed to be the same (100 mW/cm^2). Here, curve 1 is for $\theta=30°$, curve 2 is for $\theta=45°$, and curve 3 is for $\theta=60°$, where θ is complementary to the angle of deposition β.

(i) $\bar{V}_{\mathrm{och}}$ will be linearly proportional to the separation L between the electrodes and the intensity P_{in} of illumination.

(ii) $\bar{V}_{\mathrm{och}}$ will be dependent on the angle θ the grain boundaries make with the horizontal surface. It will be maximum for $\theta \sim 45°$. Besides this, $\bar{V}_{\mathrm{och}}$ will also depend on λ and T directly and also through their effects on α_λ and other parameters.

(iii) For front illumination $J_{\mathrm{scf1}} > J_{\mathrm{scb1}}$; hence, for an n-type film the polarity of $\bar{V}_{\mathrm{och}}$ is negative on the left and positive on the right. On back illumination the polarity will be reversed. For p-type films the polarity will be opposite to that of an n-type film for both front or back illumination conditions.

(iv) $\bar{V}_{\mathrm{och}}$ is dependent on the barrier height of the grain boundaries and thus the temperature behavior of the film is controlled by the barrier height V_B. Also, the activation energy for $\bar{V}_{\mathrm{och}}$ is found to be nearly equal to the barrier height, which was observed by many researchers.[13]

(v) Equation (31) shows that the $\bar{V}_{\mathrm{och}}$ increases linearly with apparent resistance of the film.

The values of $\bar{V}_{\mathrm{och}}$ have been computed for silicon films using Eq. (27) assuming the following parameters: $n_{\mathrm{is}}=10^{11}$ cm^{-2}, $L=1$ cm, $d_g=0.0001$ cm, $R_\lambda=0.3$, $t=0.0001$ cm, $\mu=10$ cm^2 V^{-1} s^{-1}, $\theta=30°$, $T=300$ K. The value of α_λ was determined using Shumka's relation.[27] The dependence of $\bar{V}_{\mathrm{och}}$ on λ (in the ~300–900 nm, range) and θ has been shown in Figs. 4 and 5, respectively.

Figure 4 depicts the variation of $\bar{V}_{\mathrm{och}}$ with wavelength λ of the incident light of 78 mW/cm^2 intensity according to Eq. (28). The curves 1, 2, and 3 have been plotted for three different values of θ, viz., 30°, 45°, and 60°, respectively. Figure 4 shows that initially $\bar{V}_{\mathrm{och}}$ increases with λ, then de-

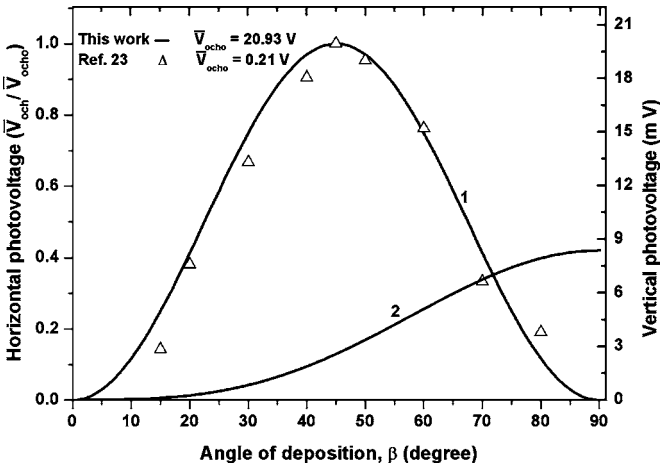

FIG. 5. Dependence of horizontal photovoltage $\bar{V}_{\rm och}$ (curve 1) and vertical photovoltage $\bar{V}_{\rm ocv}$ (curve 2) of silicon films with the angle of deposition β. Curve 1 has been plotted using Eq. (29) for $\bar{V}_{\rm och}$ and curve 2 has been plotted using Eq. (45) for $\bar{V}_{\rm ocv}$. Both curves correspond to AM 1.5 solar radiation of 78 mW/cm^2 intensity and temperature 300 K. Also, the experimental data (Δ) from Ref. 23 are reproduced and plotted in this figure. Curve 1 as well as the experimental values (Ref. 23) are normalized with respect to their values for β=45°.

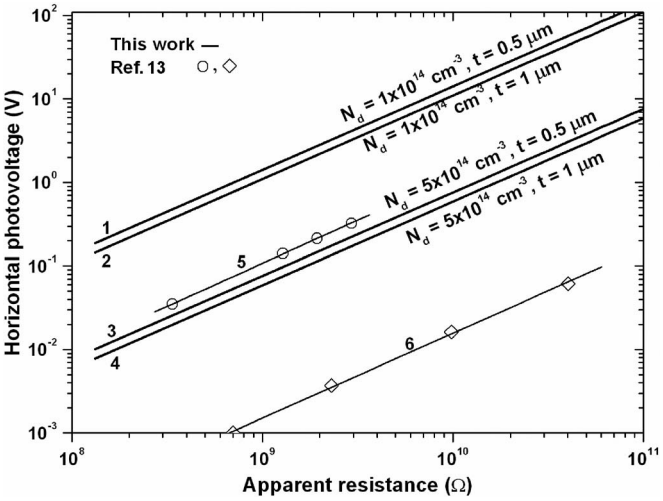

FIG. 6. Variation in photovoltage $\bar{V}_{\rm och}$ with the apparent resistance of the film (curves 1, 2, 3, and 4). Curves 1, 2, 3, and 4 have been plotted for (N_d=1×10^{14} cm^{-3}, t=0.5 μm); (N_d=1×10^{14} cm^{-3}, t=1 μm); (N_d=5×10^{14} cm^{-3}, t=0.5 μm); and (N_d=5×10^{14} cm^{-3}, t=1 μm), respectively. Some experimental data from Ref. 13 are reproduced and plotted in the figure (curves 5 and 6) for comparison.

creases after showing a peak at a certain value of λ in the visible range. The peak shifts to a shorter wavelength with an increase in θ. Such dependence of $\bar{V}_{\rm och}$ on λ was observed by Brandhorst and Potter in CdS films.[10]

Figure 5 shows the dependence of $\bar{V}_{\rm och}$ (curve 1) and $\bar{V}_{\rm ocv}$ (curve 2) on the angle of deposition β according to Eqs. (29) and (45), respectively. Theoretical values of $\bar{V}_{\rm och}$ for curve 1 have been normalized with respect to the $\bar{V}_{\rm och}$ value for β=45°. Also, the experimental values of $\bar{V}_{\rm och}$ reported by Patel and Patel[23] for $AgInTe_2$ films have been normalized and plotted in Fig. 5 for comparison with curve 1. It can be seen that both these curves match excellently. Curve 2 shows that $\bar{V}_{\rm ocv}$ is zero for β=0, i.e., for normal deposition, and keeps increasing as the angle of deposition β is increased.

The dependence of $\bar{V}_{och}$ on the apparent resistance R_a of the film is shown in Fig. 6. The values of $\bar{V}_{\rm och}$ were determined using Eq. (31) and have been plotted against R_a (curves 1, 2, 3, and 4) on a log-log scale with N_d and t as parameters. It is noted that the slope of each of these curves (1, 2, 3, and 4) is 45° from the X-axis, which shows that $\bar{V}_{\rm och}$ and R_a have a linear relationship. Two experimental $\bar{V}_{\rm och}$ vs R_a curves obtained by Brandhorst and Potter[13] for silicon films have also been plotted for comparison (curves 5, 6). Both the curves (5, 6) are parallel to the theoretical curves. This shows that Eq. (31) adequately describes the dependence of $\bar{V}_{\rm och}$ on the apparent resistance of the film.

B. General case

Equation (27) and hence Eq. (28) does not remain valid if the condition $J_{\rm sc1} \ll J_{o1}$ is not satisfied. Since $J_{\rm sc}$ increases linearly with the intensity of illumination $P_{\rm in}$, and J_{o1} decreases with a decrease in temperature T, Eq. (28) may not hold well for determining $\bar{V}_{\rm och}$ at high $P_{\rm in}$ and low T values. For such cases Eq. (26) can be used in conjunction with Eqs. (22), (18), (12), and (10). It may be pointed out that a combination of Eqs. (26), (22), (18), (12), and (10) is valid whether $J_{\rm sc1} \ll J_{o1}$ is satisfied or not, and is thus applicable even to the cases which can be described with the help of Eq. (28). In the following we discuss the cases where Eq. (26) is applied in conjunction with other equations.

1. Intensity dependence of $\bar{V}_{och}$

The dependence of $\bar{V}_{\rm och}$ on the intensity of illumination $P_{\rm in}$ in the 0–260 mW/cm^2 range has been shown in Fig. 7 (curves 1 and 2). Curves 1 and 2 have been obtained for T =302 K and T=232 K, respectively, using Eq. (26) in con-

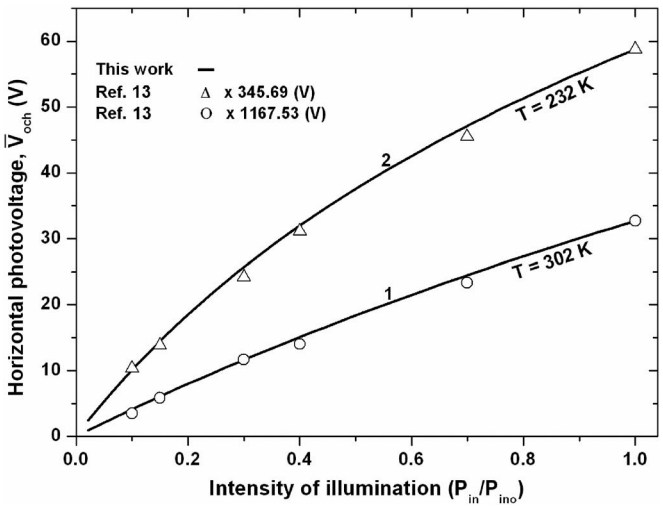

FIG. 7. Dependence of photovoltage $\bar{V}_{\rm och}$ on intensity of the incident light. Curves 1 and 2 have been plotted for the AM 1.5 solar radiation using Eq. (27) in conjunction with Eqs. (22), (18), (12), and (10). Curves 1 and 2 correspond to temperatures T=302 K and T=232 K, respectively. Experimental data from Ref. 13 for T=302 K and T=232 K are reproduced and plotted here for comparison.

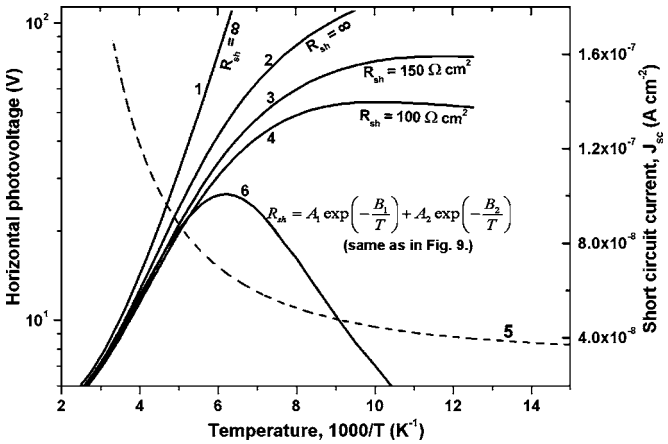

FIG. 8. Variation of the photovoltage $\bar{V}_{\rm och}$ with reciprocal temperature of the film. Curves 1 and 2 represent the ideal case where there is no shunt ($R_{\rm sh}=\infty$). Curve 1 is plotted using Eq. (27) when the condition $J_{\rm sc}\ll J_{o1}$ is satisfied. Curves 2, 3, 4, and 6 are plotted using Eqs. (26), (22), (18), (12), and (10). Curves 3 and 4 are plotted for $R_{\rm sh}=150\ \Omega\ {\rm cm}^2$ and $R_{\rm sh}=100\ \Omega\ {\rm cm}^2$, respectively, across a single GB depletion layer. Curve 6 is due to a temperature-dependent shunt resistance, $R_{\rm sh}$. Curve 5 shows the variation of $J_{\rm sc}$ with the reciprocal temperature for AM 1.5 solar radiation of 78 mW cm^{-2} intensity.

junction with Eqs. (22), (18), (12), and (10) and are plotted against the normalized intensity $P_{\rm in}/P_{{\rm in}o}$, where $P_{{\rm in}o}=260$ mW cm^{-2}. The experimental values of $\bar{V}_{\rm och}$ obtained by Brandhorst and Potter[13] for $T=302$ K and $T=232$ K, respectively, at different values of $P_{\rm in}$ in the 0 -260 mW cm^{-2} range have also been plotted in Fig. 6. It may be mentioned that experimental values are much smaller than the theoretical values to be shown in the same graph. Therefore, the experimental values for $T=302$ K and $T=232$ K are multiplied by constant factors 1167 and 346, respectively.

It can be noted that all the experimental values for $T=302$ K lie on curve 1 and all the experimental values for $T=232$ K lie on curve 2. This shows that the present model can adequately describe the intensity dependence of $\bar{V}_{\rm och}$ of obliquely deposited silicon films at different temperatures.

2. Temperature dependence of $\bar{V}_{och}$

Figure 8 shows the variation of $\bar{V}_{\rm och}$ with reciprocal temperature for silicon films. $\bar{V}_{\rm och}$ has been plotted against $1000/T$. The Y-axis is logarithmic and the X-axis is linear, so the shape of a curve actually shows the variation of $\log_{10}(\bar{V}_{\rm och})$ with $1000/T$. Curve 1 has been observed using Eq. (28). It is a straight line which shows $\log(\bar{V}_{\rm och})$ increases linearly with $1000/T$ and implies that $\bar{V}_{\rm och}$ increases exponentially with $1000/T$. Such a behavior of $\bar{V}_{\rm och}$ with temperature was observed by Brandhorst and Potter[13] in Si and SiC films above room temperature ($T>333$ K). In some Si films[13] they observed that $\bar{V}_{\rm och}$ increased more slowly with $1000/T$ as the temperature was lowered below $T<333$ K. However, in CdS films[10] and in one silicon film,[13] they found that $\bar{V}_{\rm och}$ increased with $1000/T$ for a decrease of temperature and showed a peak at ~ 250 K and then decreased rapidly with $1000/T$ for $T<250$ K. In Cd_3As_2 films, Zdanowicz *et al.*[22] had also observed a small peak of height 35 V in the $\bar{V}_{\rm och}$ vs $1000/T$ curve at ~ 240 K followed by a dip at 230 K and then a regular increase of $\bar{V}_{\rm och}$ with $1000/T$ for $230\ {\rm K}>T>90$ K. However, after storing the film for 2 days they observed a big peak of height 140 V at ~ 200 K that was followed by a sharp decrease with $1000/T$ such that $\bar{V}_{\rm och}$ was reduced to zero at 143 K and changed polarity for $T<143$ K. After storage of 3 months, films showed a still higher peak of 200 V corresponding to $T=220$ K which was followed by a sharp decrease with $1000/T$ such that $\bar{V}_{\rm och}$ again became zero at $1000/T=9$ (i.e., for $T=110$ K) and changed its polarity for $T<110$ K. These Cd_3As_2 films had been given a SiO_x coating on the film surface.

We have plotted curve 2 for the $400\ {\rm K}>T>80$ K temperature range in Fig. 8, which has been obtained using Eq. (26) in conjunction with Eqs. (22), (18), (12), and (10). It shows that $\bar{V}_{\rm och}$ increases with $1000/T$ initially sharply as T is decreased from 400 K to 350 K, and then increases more slowly with $1000/T$ for $T<350$ K but does not show any decrease in $\bar{V}_{\rm och}$ with $1000/T$. Such a behavior was also observed in two silicon films by Brandhorst and Potter[13] as mentioned above.

Thus, we find that the observed decrease of $\bar{V}_{\rm och}$ with $1000/T$ for $T<250$ K, as observed by Brandhorst and Potter in CdS films and in a Si film by Zdanowicz *et al.*[22] in Cd_3As_2 films, cannot be explained by Eqs. (26), (22), (18), (12), and (10) in the present form. In the following we analyze what additional effect, not considered so far in the derivation of some of these equations, may need to be taken into account to explain the above behavior at low temperatures.

Curve 2 mentioned above represents an ideal case where all grain boundary depletion layers have been assumed to have no leakage of charge, implying that each depletion region has an infinite shunt resistance across it. In a practical case, since a grain boundary depletion layer extends from the bulk of the film to the front exposed surface, its shunt resistance could get reduced from infinite to a finite value. For such a case we can use the following equation:

$$J_{\rm sc1}=J_{o1}\left\{\exp\left(\frac{qV_{\rm oc1}}{kT}\right)-1\right\}+\frac{V_{\rm oc1}}{R_{\rm sh}}, \tag{46}$$

instead of Eq. (18) to determine $\bar{V}_{\rm och}$ using Eq. (26) in combination with Eqs. (22), (12), and (10). In Eq. (46), $R_{\rm sh}$ is in the units of $\Omega\ {\rm cm}^2$.

Curves 3 and 4 have been plotted in Fig. 8 assuming two constant values of $R_{\rm sh}$, viz., $R_{\rm sh}=150\ \Omega\ {\rm cm}^2$ and $R_{\rm sh}=100\ \Omega\ {\rm cm}^2$, respectively. Both these curves show that $\bar{V}_{\rm och}$ increases with $1000/T$ as T decreases, and then attains a nearly constant value for further decrease in T. As expected, the values of $\bar{V}_{\rm och}$ are smaller for a smaller $R_{\rm sh}$ and are much lower than curve 2 for the same temperature range. There is also a curve 5 in Fig. 8 which shows the variation of $J_{\rm sc}$ with $1000/T$. It has been obtained using Eq. (10) and assuming α_λ to vary with T according to Shumka's relation.[27] Curve 5 shows that $J_{\rm sc}$ decreases with a decrease in T. All the curves (1, 2, 3, and 4) discussed above have been obtained using $J_{\rm sc}$

values of curve 5. Therefore, the practically observed decrease of $\bar{V}_{och}$ with T in some films cannot be accounted for by the decrease in J_{sc} value. Now it is obvious that one has to associate a temperature-dependent R_{sh} across the depletion layers of the grain boundaries of the film which have exhibited a $\bar{V}_{och}$ peak in the $\bar{V}_{och}$ vs $1000/T$ curve at a low temperature.

Apparently the origin of a shunt resistance across the depletion region of a GB should lie in the decrease in the width of the depletion region, and the depletion width should continue to decrease with lowering of the temperature to account for the decrease of R_{sh} with reciprocal temperature. This can happen if there exists a fixed charge at the surface just above the depletion region area of a nature which could attract majority carriers from the grains. In an n-type film the availability of such free electrons will try to neutralize the positively charge donors in the depletion layer around the grain boundary, leading thereby to the decrease of the width of the depletion layer.

It is known[28] that if there exists a positive charge density Q_{ox} on the surface of an n-type semiconductor, then an accumulation layer, or in other words a conducting channel, of electrons is formed in the semiconductor just below the surface. Under the steady-state condition Q_{ox} will be balanced by the equal and opposite charge in the accumulation layer of thickness t_c leading to the following relation:

$$Q_{ox} = qN_s t_c, \tag{47}$$

where N_s is the average concentration of electrons in the channel in excess of the electron density in the neutral grain and is given by the equation

$$N_s = N_D\left[\left\{\frac{kT}{q\psi_s}\left(\exp\left(\frac{q\psi_s}{kT}\right)-1\right)\right\}-1\right]. \tag{48}$$

Here, ψ_s is the surface potential due to the accumulation layer.

In the present context, it may be reasonable to assume that it is such excess carriers N_s which will be responsible for the neutralization of a fraction of the positive depletion charge in n-type films near the surface leading to creation of R_{sh} across the depletion layer of a GB under illumination. Unless all the positive charge of the depletion layer is neutralized, accumulation cannot form. However, the shunt resistance R_{sh} across a GB still having a depletion width w_{di} under illumination in the bulk, i.e., much below the surface, can be obtained using the following relation:

$$R_{sh} = \frac{w_{di}}{qN_s\mu_c}, \tag{49}$$

where w_{di} is the grain boundary depletion width under illumination and μ_c is the mobility of the electrons collected by Q_{ox}. The GB depletion width w_{di} under illumination is given by the equation

$$w_{di} = \sqrt{\frac{2\varepsilon\varepsilon_o}{qN_D}}\left[V_{BI} - \frac{kT}{q} + \frac{kT}{q}\exp\left(-\frac{qV_{BI}}{kT}\right)\right]^{1/2}, \tag{50}$$

where V_{BI} is the barrier height of the grain boundary under illumination. Equation (48) shows that, for a given Q_{ox}, N_s increases with a decrease in temperature, and this makes R_{sh} decrease with a decrease in temperature.

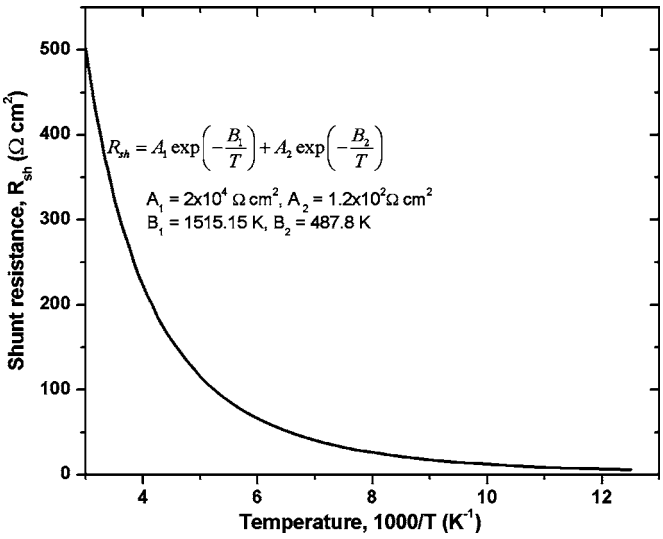

FIG. 9. Variation of the shunt resistance, R_{sh}, across a grain boundary depletion layer of an n-type silicon film with the reciprocal temperature. The curve is plotted for a positive surface charge density $Q_{ox}=1.6\times10^{-12}$ C/cm^2. Electron mobility is considered to vary with temperature as $\mu_c = aT^{-2.42}$, where $a=2.8\times10^6$ cm^2 V^{-1} s^{-1} K$^{2.42}$.

We have used Eq. (49) to determine R_{sh} as a function of temperature in the range 400 K$>T>$80 K for silicon films assuming $Q_{ox}=8\times10^{-12}$ C cm^{-2}, and have plotted it in Fig. 9. The mobility μ_c has been considered to vary as $\mu_c = aT^{-2.42}$, where $a=2.8\times10^6$ cm^2 V^{-1} s^{-1} K$^{2.42}$. Figure 9 shows that the shunt resistance decreases with a decrease in T rapidly, and its temperature dependence in the 300 K $<T<$80 K range can be described by the equation

$$R_{sh} = A_1\exp(-B_1/T) + A_2\exp(-B_2/T), \tag{51}$$

where A_1, A_2 and B_1, B_2 are constants and have values of $A_1=2\times10^4$ Ω cm^2, $A_2=1.2\times10^2$ Ω cm^2, $B_1=1515$ K, and $B_2=488$ K, respectively.

Again, in Fig. 8, a curve 6 has been drawn assuming R_{sh} varies with T according to Eq. (51) for 300 K$>T>$80 K. This curve 6 of Fig. 8 shows that $\bar{V}_{och}$ increases with $1000/T$, while lowering of T shows a peak at $T=158$ K, which then decreases with a further decrease of T. Thus, the curve 6 of Fig. 8 explains the existence of a peak in the $\bar{V}_{och}$ with $1000/T$ at low temperature in silicon films, and indicates that films showing such behavior must acquire a surface charge Q_{ox} of polarity the same as the depletion layer charge (i.e., a positive Q_{ox} for n-type films and a negative Q_{ox} for p-type films) during preparation, illumination, cooling to low temperatures, storage of the films in an ambient, or any other treatment to which they may be subjected.

C. Related effects

1. Current and voltage transient effects

Brandhorst and Potter[13] had found that, when a small voltage (~0.5 V) was applied across the horizontal electrodes of the film in the dark, the current decreased exponentially, and after removal of the bias the films were observed

to retain a voltage which decayed exponentially with time.[13] They attributed the transient behavior of the current and voltage to induction of a space charge in the film on application of the bias. However, they did not explain how the space charge could have been induced.

The present model assumes that there already exists a space-charge layer in the form of a double depletion layer under thermal equilibrium due to the trapping of majority carriers at a grain boundary from the adjacent grains. The trapping of carriers at the trap levels associated with the grain boundary and the emission of the trapped carriers from the traps to the conduction or the valence band goes on all the time and the trapping and emission rates are equal under thermal equilibrium condition. However, the two rates become unequal immediately after a voltage is applied or removed from across a grain boundary. When voltage is applied across a grain boundary then one side of the grain boundary becomes forward biased and the other side becomes reverse biased, as described by Singh *et al.*[26] and also by Groot and Card.[29] As a result of the forward bias, the majority carriers are injected into the grain boundary and starts getting trapped at the grain boundary, as explained by Broniatowski in a deep-level transient spectroscopy (DLTS) study of grain boundaries.[30] This process is like the charging of a capacitor. Hence, soon after the application of a dc bias the current across the grain boundary decreases with time generally exponentially when carrier trapping is going on, and attains a saturation value after a certain time when no more carriers can be trapped at the grain boundary. When the bias is removed the accumulated additional charge still present at the grain boundary gives rise to a voltage across the grain boundary. This voltage decays slowly until all the excess trapped charge is emitted as free carriers by a thermally activated process. For a single dominant trap level the decay is usually exponential.[31] Thus, the application and removal of a bias across a grain boundary or between contacts on the films having such grain boundaries leads to the current and the voltage transients, respectively. So, the current and voltage transients as observed in obliquely deposited films by Brandhorst and Potter[13] can be understood well with the help of a grain boundary model.

2. Role of non-electrically active grain boundaries

All grain boundaries along the horizontal are in series, so no grain boundary, however weak, is likely to short-circuit the effect of another grain boundary. If we consider that some of the grain boundaries, say n_{L1} out of n_L, do not contribute to the photovoltage, then $\bar{V}_{\rm och}$ will be reduced by an amount $n_{L1}V_{\rm oc1}$ if they are bunched together. However, a non-electrically active (or inactive) grain boundary can make some difference to the photovoltage being produced by an adjacent electrically active grain boundary by effectively enhancing d_g if it lies between the two active grain boundaries.

3. Films with thickness gradient

Strictly speaking, the present model is expected to be valid for the obliquely deposited films of uniform thickness, or, in other words, for the films having an insignificant thickness gradient. In many cases the obliquely deposited films may be significantly thicker at the end that is nearer to the source than the far end. For such a case the model may be applied by assuming the film thickness to vary in a staircase fashion from one electrode to the other, and considering the film to be made up of many identical segments each of uniform length ΔL. We assume that the thickness of the first segment at the thinner end is Δt; then, the second segment of length ΔL will be of thickness $2\Delta t$ and the third one of thickness $3\Delta t$. If there are m such segments between the electrodes, then the thickness of the mth segment would be $m\,\Delta t$. Now we can apply Eq. (27) to each of these segments and determine the photovoltage across each segment. For instance, to apply Eq. (27) to the second segment one would need to replace L by ΔL and t by $2\Delta t$. We denote the photovoltages developed across the first, second,…,mth segments by $\bar{V}_{\rm och1}$, $\bar{V}_{\rm och2}$,…,$\bar{V}_{{\rm och}m}$, respectively. Since the horizontal photovoltages are in series, the resultant photovoltage between the film electrodes will be the sum of the photovoltages of all the segments and will be given by

$$\bar{V}_{\rm och} = \bar{V}_{\rm och1} + \bar{V}_{\rm och2} + \cdots + \bar{V}_{{\rm och}m}. \tag{52}$$

In this way Eq. (28) or other equations can be applied to films with thickness gradients.

IV. CONCLUSION

We have developed a phenomenological model of photovoltage in obliquely deposited semiconductor films on transparent substrates assuming that the grains and grain boundaries are inclined at an angle θ from the horizontal, and that there exists a double potential barrier at the GB due to the trapping of majority carriers. On normal illumination with radiation of high absorption coefficient in the semiconductor there is a larger absorption of photons on the front side of a grain boundary than on the back side, and this gives rise to a net photocurrent $J_{\rm sc1}$ and a photovoltage $V_{\rm oc1}$. A large photovoltage $\bar{V}_{\rm och}$ is generated between two electrodes on the horizontal plane because there are a large number of grain boundaries between them. For low intensity, when $J_{\rm sc1} \ll J_{o1}$, $\bar{V}_{\rm och}$ is given by Eq. (29). Then, $\bar{V}_{\rm och}$ is linearly proportional to the distance L between the electrodes, the apparent resistivity ρ_a of the film, and the intensity of illumination $P_{\rm in}$. $\bar{V}_{\rm och}$ is dependent on the angle of deposition β. For small-grain films $\bar{V}_{\rm och}$ is proportional to $\sin^2 2\beta$ and is maximum for $\beta = 45°$. For higher intensities or lower temperatures $\bar{V}_{\rm och}$ increases more slowly with $P_{\rm in}$ and reciprocal temperature than expected on the basis of Eq. (29). This is because in such cases the condition $J_{\rm sc} \ll J_{o1}$ is no longer valid. Then, $\bar{V}_{\rm och}$ can be determined using Eq. (26) in combination with Eqs. (22), (18), (12), and (10). $\bar{V}_{\rm och}$ normally increases with reciprocal temperature initially as the temperature is decreased from the room-temperature value. However, the increase of $\bar{V}_{\rm och}$ with the reciprocal temperature becomes slower at low temperatures. $\bar{V}_{\rm och}$ becomes smaller and attains a nearly constant value at low temperatures if the shunt resistance $R_{\rm sh}$ of the grain boundary depletion layer has a constant finite value. On the other hand, if

there exists a fixed charge Q_{ox} at the surface of the film having the same polarity as the grain boundary depletion layer charge (i.e., if Q_{ox} is positive for *n*-type film and is negative for *p*-type films), then R_{sh} becomes temperature dependent and decreases with the lowering of the temperature. In such obliquely deposited films, $\bar{V}_{och}$ decreases rapidly with a decrease in temperature after having attained a peak value.

The photovoltage $\bar{V}_{ocv}$ across the film thickness is given by Eq. (45). It also increases with the apparent resistance of the film and the intensity of illumination. $\bar{V}_{ocv}$ is negligible for the normal deposition of the film (i.e., $\beta=0$), but increases progressively for oblique deposition as the angle of deposition β is increased in the $0<\beta<90°$ range.

ACKNOWLEDGMENTS

We are thankful to Dr. Vikram Kumar, Director National Physical Laboratory, New Delhi for his permission to publish this work. One of the authors, Dinesh Kumar, wishes to thank University Grant Commission, India for providing financial support to him during this work.

[1]J. Starkiewicz, L. Sosnowski, and O. Simpson, Nature (London) **158**, 26 (1946).
[2]R. Y. Berlaga and L. P. Strakhov, Zh. Tekh. Fiz. **24**, 943 (1954).
[3]R. Y. Berlaga, M. A. Rumsh, and L. P. Strakhov, Zh. Tekh. Fiz. **25**, 195 (1878).
[4]G. Schwabe, Z. Naturforsch. A **10A**, 78 (1955).
[5]T. Piwkowski, Acta Physiol. Pol. **15**, 271 (1956).
[6]L. Pensak, Phys. Rev. **109**, 601 (1958).
[7]B. Goldstein, Phys. Rev. **109**, 601 (1958).
[8]B. Goldstein and L. Pensak, J. Appl. Phys. **30**, 155 (1959).
[9]M. Kamiyama, M. Haradome, and H. Kukimoto, Jpn. J. Appl. Phys. **1**, 202 (1962).
[10]H. W. Brandhorst, Jr., F. L. Acampora, and A. E. Potter, J. Appl. Phys. **39**, 6071 (1968).
[11]S. G. Ellis, F. Hermann, E. E. Loebner, W. J. Merz, C. W. Struck, and J. G. White, Phys. Rev. **109**, 1860 (1958).
[12]H. Kallmann, B. Kramer, E Haidemenakis, W. J. Mc Aleer, H. Barkemeyer, and P. I. Pollak, J. Electrochem. Soc. **108**, 247 (1961)
[13]H. W. Brandhorst and A. E. Potter, J. Appl. Phys. **35**, 1997 (1964).
[14]S. Martinuzzi, Compt. Rend. **258**, 1764 (1964).
[15]G. Cheroff and S. P. Keller, Phys. Rev. **111**, 98 (1958).
[16]W. I. Merz, Helv. Phys. Acta **31**, 625 (1958).
[17]A. Lempicki, Phys. Rev. **113**, 1204 (1959).
[18]G. F. Neumark, Phys. Rev. **125**, 838 (1962).
[19]P. P. Konorov and K. Liubits, Sov. Phys. Solid State **6**, 55 (1964).
[20]M. Takahasi and J. Nakai, Jpn. J. Appl. Phys. **3**, 364 (1964).
[21]K. L. Chopra, *Thin Film Phenomena* (McGraw-Hill, New York, 1969), p. 177.
[22]L. Zdanowicz, A. Sas, and B. Dzido, Thin Solid Films **36**, 269 (1976).
[23]S. M. Patel and B. H. Patel, Thin Solid Films **173**, 916 (1989).
[24]S. K. Sharma and R. S. Srivastava, Thin Solid Films **150**, 217 (1987).
[25]J. Y. W. Seto, J. Appl. Phys. **46**, 5247 (1975).
[26]S. N. Singh, R. Kishore, and P. K. Singh, J. Appl. Phys. **57**, 2793 (1985).
[27]A. Shumka, in Proceedings of the Eighth Photovoltaic Specialist Conference, Seattle, IEEE, 1970, Vol. 96.
[28]S. M. Sze, *Physics of Semiconductor Devices* (Wiley and Sons, Singapore, 2002), pp. 248–366.
[29]A. W. De Groot and H. C. Card, IEEE Trans. Electron Devices **ED-31**, 1365 (1984).
[30]A. Broniatowski, Phys. Rev. B **36**, 5895 (1987).
[31]C. H. Seager, G. E. Pike, and D. S. Ginley, Phys. Rev. Lett. **43**, 532 (1979).